Transistorlike Device for Heating and Cooling Based on the Thermal Hysteresis of VO_2

Jose Ordonez-Miranda,* Younès Ezzahri, Jérémie Drevillon, and Karl Joulain

Institut Pprime, CNRS, Université de Poitiers, ISAE-ENSMA, F-86962 Futuroscope Chasseneuil, France

(Received 25 May 2016; revised manuscript received 29 August 2016; published 7 November 2016)

We demonstrate that a far-field transistor made up of a phase-change material base with thermal hysteresis can efficiently be used as a thermal device capable of heating and cooling. Based on the principle of energy conservation for the heat currents by radiation, conduction, and convection, it is shown that the base temperature undergoes significant jumps as the transistor amplification factor is optimized. When the collector and emitter of the transistor operate at 350 and 300 K, respectively, a temperature jump of +18 K (−5 K) is obtained during the heating (cooling) of a VO_2 base excited with 208 $W\,m^{-2}$ (63 $W\,m^{-2}$). These significant jumps are mainly driven by the photon heat current and could open new perspectives on thermal machines.

DOI: 10.1103/PhysRevApplied.6.054003

I. INTRODUCTION

Since the conception of the thermal diode [1–3] and thermal transistor [4–7] by heat conduction and heat radiation, over the last few years, significant research effort has been dedicated to guide, amplify, and control thermal currents, in a similar way as is done with electrical thermal currents, through the electronic diode and transistor. The role of the electrical potential and currents in electronics is played by thermostats and heat fluxes in these thermal devices, which could be used as the basic building blocks for thermal circuits [8], thermal logic gates [9], thermal memories [10–12], and quantum rectification [13].

Thermal rectifiers allowing the heat-flux exchange between two diode terminals in one direction and blocking it when their temperatures are interchanged, were theoretically proposed based on phononic [1,14–19] and electronic [20] heat conduction. This rectification effect can also be obtained by photons [2,21–25] and was experimentally observed in carbon nanotube structures [26], semiconductor quantum dots [27], bulk oxide materials [28], and vanadium dioxide (VO_2) [29,30], which has recently attracted a lot of interest due to its dielectric-to-metal transition at temperatures near room one [31]. The heat flux can be enhanced with VO_2 in the dielectric phase and suppressed when it becomes metallic [32], which results in thermal rectification close to unity [3,33,34]. VO_2 and other phase-change materials (PCMs) were also used to develop the radiative thermal transistor, in both the near [5] and far [7] fields. This three-terminal device consists of a VO_2 base placed in between two thermostats playing the roles of a thermal collector and emitter, which exchange a heat flux that can be switched, amplified, and modulated by a tiny action on the base temperature, inside the VO_2 phase transition zone. In these two latter works, fine heat-flux control with amplification factors higher than 10 were reported, however, none of them put so much attention on either the intrinsic thermal hysteresis of VO_2 or the temperature control, which are considered in the present work.

The objective of this paper is to theoretically demonstrate that a thermal transistor with a PCM base can be used as a thermal device for heating and cooling. This is done by taking into account the heat currents by radiation, conduction, and convection; and exploiting the effect of PCM thermal hysteresis on the heat fluxes that the base exchanges with the collector and emitter. We show that these heat fluxes and the base temperature undergo jumps under a small modification of the heat flux applied to the base.

II. THEORETICAL MODELING

Let us consider a far-field transistor composed of a PCM placed between two bodies set at temperatures T_1 and T_2 ($T_1 > T_2$), as shown in Fig. 1. By analogy to the electronic bipolar transistor, these latter bodies stand for the collector and the emitter of the thermal transistor, while the base is the PCM, whose gray emissivity $\varepsilon(T)$ changes with its temperature T that is driven by the external heat flux ϕ_3. The heat flux ϕ_1 (ϕ_2) exchanged by the collector (base) and the base (emitter) is given by

$$\phi_1 = \sigma\varepsilon_e(T)(T_1^4 - T^4) + G(T_1 - T), \tag{1a}$$

$$\phi_2 = \sigma\varepsilon_e(T)(T^4 - T_2^4) + G(T - T_2), \tag{1b}$$

where $\sigma = 5.67 \times 10^{-8}\ W\,m^{-2}\,K^{-4}$ is the Stefan-Boltzmann constant, the effective emissivity $\varepsilon_e(T) = [1/\varepsilon(T) + 1/\varepsilon_0 - 1]^{-1}$, and the conductance $G = (2/h + L/k)^{-1}$, ε_0 being the emissivity of the facing walls of the collector and emitter, which exchange heat by

*jose.ordonez@cnrs.pprime.fr

convection with the intracavity gas of thermal conductivity k and heat transfer coefficient h. For air, $k = 25\,\mathrm{mW\,m^{-1}\,K^{-1}}$ and $h = 5\ \mathrm{W\,m^{-2}\,K^{-1}}$, within a wide range of temperatures [35]. The principle of energy conservation establishes that these two heat fluxes are related to the applied one by $\phi_3 = \phi_2 - \phi_1$, which yields

$$\phi_3 = 2\sigma\varepsilon_e(T)(T^4 - T_e^4) + 2G(T - T_m), \tag{2}$$

where $T_e = \sqrt[4]{(T_1^4 + T_2^4)/2}$ and $T_m = (T_1 + T_2)/2 \leq T_e$ are the equilibrium temperatures ($\phi_3 = 0$) of the base, in the absence of conduction and convection ($G = 0$) and radiation ($\varepsilon_e = 0$), respectively. ϕ_3 can uniformly be injected into the VO_2 base by coating its top surface with a paint opaque to an incident laser beam, as is usually done in photothermal experiments [36], or by applying a voltage difference through a couple of electrodes placed on the top and bottom surfaces of the base, as was previously proposed [5]. Equation (2) establishes that a variation of the applied flux ϕ_3 induces the change of the PCM temperature T, which drives the fluxes ϕ_1 and ϕ_2 through Eqs. (1a) and (1b), respectively. This heat-flux modulation can be used to generate a transistor effect characterized by the amplification factor $\alpha = \partial\phi_2/\partial\phi_3$, which yields

$$2\alpha = \frac{\varepsilon_e'(T)(T^4 - T_2^4) + 4\varepsilon_e(T)T^3 + G/\sigma}{\varepsilon_e'(T)(T^4 - T_e^4) + 4\varepsilon_e(T)T^3 + G/\sigma}, \tag{3}$$

where $\varepsilon_e'(T) = d\varepsilon_e(T)/dT$. According to Eqs. (2) and (3), the amplification factor associated with the flux ϕ_1 is $\partial\phi_1/\partial\phi_3 = \alpha - 1$, and so we will only focus on α. Given that $\alpha = 1/2$, outside the transition region [$\varepsilon_e'(T) = 0$], it is clear that the possible heat-flux amplification is the result of the temperature-dependent emissivity $\varepsilon_e(T)$, within the transition region of the PCM base. Note that α diverges at the temperature $T = T_c$, for which the denominator of Eq. (3) reduces to zero. This singular behavior corresponds to $(\partial T/\partial\phi_3)^{-1} = 0$, which indicates that an infinitely small change on ϕ_3 induces a much larger variation of T, around T_c. In practice, however, the changes of ϕ_3 can only be done in finite steps and therefore the values of α are expected to remain finite but maximized at a base temperature T_c given by

$$\varepsilon_e'(T_c)(T_c^4 - T_e^4) + 4\varepsilon_e(T_c)T_c^3 + G/\sigma = 0. \tag{4}$$

The existence of the critical temperature T_c [numerical solution of Eq. (4)] thus establishes that it is possible to optimize α by tuning the base temperature equal to or close to T_c, which is $T_c > T_e$ ($T_c < T_e$), for $\varepsilon_e'(T_c) < 0$ [$\varepsilon_e'(T_c) > 0$]. According to Eqs. (1) and (2), the flux ϕ_3 required to reach this temperature and the associated fluxes ϕ_2 and ϕ_1 are determined by

$$\phi_{3c} = -8\sigma\frac{\varepsilon_e^2(T_c)}{\varepsilon_e'(T_c)}T_c^3 + 2G\left(T_c - T_m - \frac{\varepsilon_e(T_c)}{\varepsilon_e'(T_c)}\right), \tag{5a}$$

$$2\phi_{2c} = \sigma\varepsilon_e(T_c)(T_1^4 - T_2^4) + G(T_1 - T_2) + \phi_{3c}, \tag{5b}$$

$$2\phi_{1c} = \sigma\varepsilon_e(T_c)(T_1^4 - T_2^4) + G(T_1 - T_2) - \phi_{3c}, \tag{5c}$$

where $\phi_{nc} = \phi_n(T_c)$, for $n = 1, 2, 3$. Equation (5a) indicates that, for pure heat radiation ($G = 0$), the tuning of T_c is only possible ($\phi_{3c} > 0$) when the emissivity slope is negative, while the heat conduction and convection opens the possibility of using a PCM with $\varepsilon'(T_c) > 0$. In both cases, Eq. (5a) shows that faster phase transitions (steeper emissivity slopes) require smaller heat-flux excitations for reaching T_c. Given that $T_1 > T_2$, Eqs. (5a)–(5c) show that the heat flux $\phi_{2c} > \phi_{1c}$ and keeps flowing from the base to the emitter. This is not the case of ϕ_{1c}, which can (be negative and) change its direction and go from the base to the collector for a high-enough ϕ_{3c}.

Temperatures T_{CB} and T_{BE} within the collector-base (CB) and base-emitter (BE) gas cavities are determined by Fourier's law, as follows: $T_n(z) = A_n + B_n z$, where z is the position and A_n and B_n are constants that depend on the continuity of the temperature and heat flux ψ_n by conduction and convection, for $n = \mathrm{CB}$ and BE. Under the coordinates system shown in Fig. 1, these standard boundary conditions read

$$T_{\mathrm{CB}}(z_1 = 0) = T_1, \tag{6a}$$

$$T_{\mathrm{CB}}(z_1 = L) = T_{\mathrm{BE}}(z_2 = 0) = T, \tag{6b}$$

$$T_{\mathrm{BE}}(z_2 = L) = T_2, \tag{6c}$$

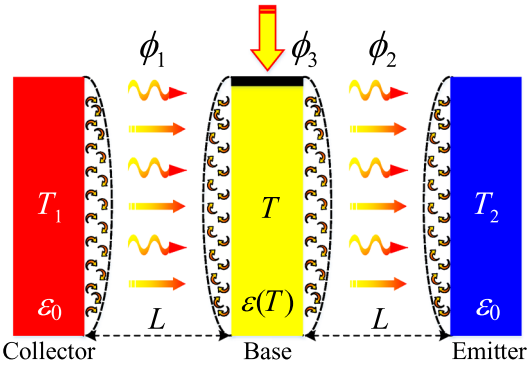

FIG. 1. Scheme of a thermal transistor made up of a PCM at temperature T and placed between two thermostats at temperatures T_1 and T_2. The round, straight, and wavy arrows stand for heat convection, conduction, and radiation, respectively. The dashed lines represent the limits of the thermal boundary layers in the vicinity of the bounding surfaces.

$$h[T_1 - T_{CB}(\delta)] = \frac{k}{L-2\delta}[T_{CB}(\delta) - T_{CB}(L-\delta)] = h[T_{CB}(L-\delta) - T], \quad (6d)$$

$$h[T - T_{BE}(\delta)] = \frac{k}{L-2\delta}[T_{BE}(\delta) - T_{BE}(L-\delta)] = h[T_{BE}(L-\delta) - T_2], \quad (6e)$$

where δ is the average thickness of the convection boundary layer alongside the collector, base, and emitter surfaces. The eight conditions in Eqs. (6a)–(6e) together with the temperature continuity at the four interfaces $z_1 = \delta,\ L-\delta$ and $z_2 = \delta,\ L-\delta$, yield the following temperature profiles:

$$T_{CB}(z_1) = T_1 - \frac{T_1 - T}{2 + N_u} \times \begin{cases} \frac{z_1}{\delta}, & 0 \le z_1 \le \delta \\ 1 + N_u \frac{z_1 - \delta}{L-2\delta}, & \delta \le z_1 \le L-\delta \\ 2 + N_u + \frac{z_1 - L}{\delta}, & L-\delta \le z_1 \le L \end{cases} \quad (7)$$

$$T_{BE}(z_2) = T - \frac{T - T_2}{2 + N_u} \times \begin{cases} \frac{z_2}{\delta}, & 0 \le z_2 \le \delta \\ 1 + N_u \frac{z_2 - \delta}{L-2\delta}, & \delta \le z_2 \le L-\delta \\ 2 + N_u + \frac{z_2 - L}{\delta}, & L-\delta \le z_2 \le L \end{cases} \quad (8)$$

where $N_u = h(L-2\delta)/k$ is the Nusselt number characterizing the heat convection and heat conduction inside the gas cavities. For the natural convection considered here, typical values of δ are smaller than 1 mm ($\delta < 1$ mm) [35], and therefore its contribution to N_u becomes negligible for a cavity thickness $L > 1$ cm. For an air cavity with $L = 10$ cm, the number $N_u = 20$ indicates that the heat convection flow is in the laminar wave-free regime [35].

III. RESULTS AND DISCUSSION

The temperature and heat fluxes involved in the thermal transistor shown in Fig. 1 are now analyzed for a base of VO_2. This PCM is not gray, however, its mean emissivity ε over all spectral wavelengths of radiation is able to provide a fairly good description of the heat transport in a far-field transistor [37]. The collector and emitter are treated as blackbodies ($\varepsilon_0 = 1$), and their distance to the base is taken $L = 10$ cm ($G = 2.5\ \mathrm{W\,m^{-2}\,K^{-1}}$). All calculations are done for $T_2 = 300$ K.

The temperature dependence of the mean emissivity ε of VO_2 is shown in Fig. 2, for both its heating and cooling regimes. The dots stand for experimental data [38,39] and the heating line represents the prediction of the Bruggemann model [39]. The cooling curve is a downward

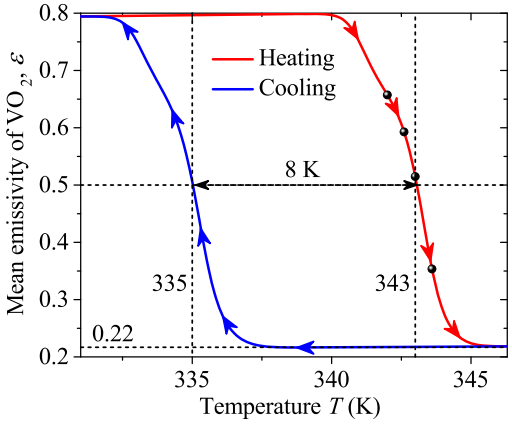

FIG. 2. Mean emissivity of VO_2 vs temperature.

shift of the heating one by 8 K, due to the thermal hysteresis observed by Qazilbash *et al.* [39]. For both transitions, $0.22 \le \varepsilon \le 0.79$ remains bounded between its values for the metallic and dielectric phases.

Figures 3(a) show the evolution of the VO_2 base temperature T with the applied heat flux ϕ_3. Note that the generally linear behavior of T with ϕ_3 disappears for temperatures within the VO_2 transition regions shown in

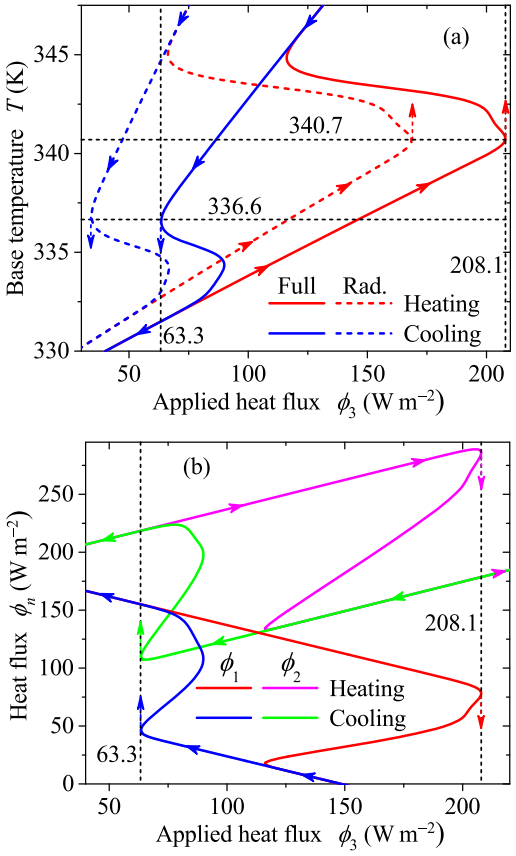

FIG. 3. (a) VO_2-base temperature T and (b) heat fluxes ϕ_1 and ϕ_2 as functions of ϕ_3. Calculations are done for $(T_1, T_2) = (350, 300)$ K, and the arrows indicate the behaviors during the base heating and cooling.

Fig. 2. When the VO_2 base is heated through a continuous increase of ϕ_3, there exists a critical ϕ_3 defined by $(\partial T/\partial\phi_3)^{-1} = 0$, for which the temperature jumps from $T = T_c^>$ to a higher value. On the other hand, when the base is cooled down by decreasing ϕ_3, its temperature undergoes another jump from $T = T_c^<$ given by $(\partial T/\partial\phi_3)^{-1} = 0$, to a lower one. These critical temperatures $T_c^>$ and $T_c^<$ are associated with the dielectric-to-metal and metal-to-dielectric phase transitions of VO_2, respectively, such as the intermediate temperatures $T_c^< < T < T_c^>$, and they are not reachable by either the heating or the cooling regimes. This thermal bistability shows up due to the competing effects of the increase of T^4 and the decrease of $\varepsilon(T)$, as T raises and vice versa [see Eq. (2a)], and it was experimentally observed in a two-terminal VO_2 device [12,40]. In our three-terminal device, these temperature jumps increase as the equilibrium temperature T_e reduces. They can be as high as 45 K (20 K) during the heating (cooling) and, therefore, they can be used to heat up or cool down the VO_2 base with a minimal change of ϕ_3. The existence of these two temperature jumps is totally due to the temperature dependence of the PCM emissivity ε, as indicated by Eq. (4), but their values are determined by the thermal hysteresis of ε. This hysteresis along with the combined effect of the thermal radiation, conduction, and convection drive the VO_2 base temperature, and they represent the main differences of the present work with respect to our previous one [25], developed for a transistor in vacuum. Furthermore, note that the temperature jumps can even be enhanced by reducing the conduction and convection conductance G, as shown in Fig. 4 by the lines obtained for heat radiation.

According to Fig. 3(a), the temperature jump $\Delta T^>$ ($\Delta T^<$), shown in Fig. 4 for the heating (cooling) of the transistor base, is given by

$$\Delta T^> = T_{\max} - T_c^>, \tag{9a}$$

$$\Delta T^< = T_c^< - T_{\min}, \tag{9b}$$

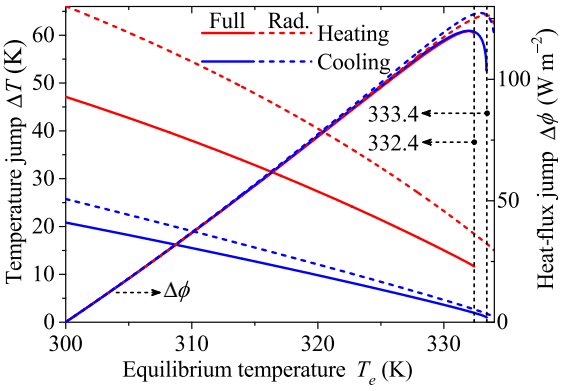

FIG. 4. Temperature and heat-flux jumps as a function of the equilibrium temperature T_e.

where $T_{\max}$ and $T_{\min}$ are defined by $\phi_3(T_{\max})|_{\varepsilon=\varepsilon_m} = \phi_3(T_c^>)$ and $\phi_3(T_{\min})|_{\varepsilon=\varepsilon_d} = \phi_3(T_c^<)$, ε_m and ε_d being the emissivity of the PCM in the metallic and dielectric phases, respectively. By combining these relations with Eqs. (2), (4), and (5a), one obtains

$$T_{\max}^4 - (T_c^>)^4 + a_m(T_{\max} - T_c^>) + b_m = 0, \tag{10a}$$

$$T_{\min}^4 - (T_c^<)^4 + a_d(T_{\min} - T_c^<) + b_d = 0, \tag{10b}$$

where the parameters a_n and b_n for $n = m, d$, are defined by

$$a_n = \frac{G}{\sigma\varepsilon_n}, \tag{11a}$$

$$b_n = \frac{\varepsilon(T_c) - \varepsilon_n}{\varepsilon'(T_c)}\left(a_n + 4\sigma\frac{\varepsilon(T_c)}{\varepsilon_n}T_c^3\right), \tag{11b}$$

with $T_c = T_c^>$ ($T_c = T_c^<$), when $n = m$ ($n = d$). Taking into account that $\varepsilon_m < \varepsilon(T_c) < \varepsilon_d$, Eqs. (12a)–(13b) indicate that $T_{\max} > T_c^>$ and $T_{\min} < T_c^<$ for a PCM with $\varepsilon'(T_c) < 0$, as is the case of VO_2 (see Fig. 2). In the absence of heat conduction and convection ($G = 0$), the solutions of Eqs. (12a) and (12b) are the simple expressions $T_{\max} = \sqrt[4]{(T_c^>)^4 - b_m}$ and $T_{\min} = \sqrt[4]{(T_c^<)^4 - b_d}$. For $G > 0$, on the other hand, both Eqs. (12a) and (12b) can conveniently be expressed as

$$x^4 + a_n x = c_n, \tag{12a}$$

$$c_n = T_c^4 + a_n T_c - b_n, \tag{12b}$$

where $x = T_{\max}$ ($x = T_{\min}$), for $n = m$ ($n = d$). The physical solution ($x > 0$) of Eq. (14a) is

$$x = \sqrt{\frac{y}{2}}\left(\sqrt{\frac{a_n}{y\sqrt{2y}} - 1} - 1\right), \tag{13a}$$

$$y = y_+ + y_-, \tag{13b}$$

$$y_\pm = \sqrt[3]{\left(\frac{a_n}{4}\right)^2 \pm \sqrt{\left(\frac{a_n}{4}\right)^4 + \left(\frac{c_n}{3}\right)^3}}. \tag{13c}$$

Equations (11a)–(13c) indicate that the temperature jumps increase with the steepness of the PCM emissivity slope $[\varepsilon'(T_c)]$ at the critical temperature, and therefore the temperature jumps shown in Fig. 4 could be amplified by replacing the VO_2 with another PCM with a faster phase transition on its emissivity.

The sudden temperature changes induce jumps on the heat fluxes ϕ_1 and ϕ_2, as shown in Fig. 3(b). These jumps occur at the same ϕ_3 as those of the base temperature, such that the decrease of ϕ_1 and ϕ_2 during the heating is exactly

compensated by their corresponding increase for the cooling, due to the thermal hysteresis of the VO_2 emissivity. Furthermore, during the heating or cooling regime and for a fixed ϕ_3, the jump $\Delta\phi_1$ of ϕ_1 is equal to the one $\Delta\phi_2 = \Delta\phi_1 = \Delta\phi$ of ϕ_2, as established by the principle of energy conservation ($\phi_2 = \phi_1 + \phi_3$). This $\Delta\phi$ increases almost linearly with T_e, is practically the same for both the heating and cooling, and it can be slightly enhanced with pure heat radiation ($G = 0$), as shown in Fig. 4. To quantify $\Delta\phi$, note that the jump $\Delta\phi_j^>$ ($\Delta\phi_j^<$) of the heat flux ϕ_j during the heating (cooling) of the transistor base, is defined by

$$\Delta\phi_j^> = \phi_j(T_c^>) - \phi_j(T_{\max}), \tag{14a}$$

$$\Delta\phi_j^< = \phi_j(T_{\min}) - \phi_j(T_c^<), \tag{14b}$$

where $j = 1, 2$. By using the definition of $\phi_1^<$ in Eq. (1a) and the continuity of ϕ_3, when the base temperature changes from $T_c^>$ ($T_c^<$) to $T_{\max}$ ($T_{\min}$), one obtains

$$2\phi_1(T_{\max}) = \sigma\varepsilon_m(T_1^4 - T_2^4) + G(T_1 - T_2) - \phi_{3c}(T_c^>), \tag{15a}$$

$$2\phi_1(T_{\min}) = \sigma\varepsilon_d(T_1^4 - T_2^4) + G(T_1 - T_2) - \phi_{3c}(T_c^<). \tag{15b}$$

After inserting Eq. (5a) into Eqs. (15a) and (15b), one finds that the heat-flux jumps are driven by the heat flux exchanged by the collector and emitter via the base, as follows:

$$2\Delta\phi_1^> = \sigma[\varepsilon(T_c^>) - \varepsilon_m](T_1^4 - T_2^4), \tag{16a}$$

$$2\Delta\phi_1^< = \sigma[\varepsilon_d - \varepsilon(T_c^<)](T_1^4 - T_2^4). \tag{16b}$$

Note that the contribution of heat conduction and convection ($G > 0$) on $\Delta\phi_1^>$ ($\Delta\phi_1^<$) appears implicitly through the critical temperature $T_c^>$ ($T_c^<$), which is defined in Eq. (4). However, this contribution only changes slightly the critical temperature, as shown in Fig. 5 and therefore the impact of the heat conduction and convection on the heat-flux jumps is generally weak. According to the relation $\varepsilon = \varepsilon[T(\phi_3)]$ given by Eq. (2), the emissivity $\varepsilon(T_c^>)$ [$\varepsilon(T_c^<)$] is smaller (bigger), but very close to ε_d (ε_m). We thus have $\varepsilon(T_c^>) \approx \varepsilon_d$ and $\varepsilon(T_c^<) \approx \varepsilon_m$, and therefore $\Delta\phi_1^> \approx \Delta\phi_1^<$, as shown in Fig. 4. On the other hand, the jumps $\Delta\phi_2^>$ and $\Delta\phi_2^<$, defined in Eqs. (14a) and (14b) for the heat flux ϕ_2, can be determined by following a similar procedure to the one done for ϕ_1, or more directly, by applying the principle of energy conservation ($\phi_2 = \phi_1 + \phi_3$). For instance, $\Delta\phi_2^> = \phi_2(T_c^>) - \phi_2(T_{\max}) = \phi_1(T_c^>) + \phi_3(T_c^>) - \phi_1(T_{\max}) - \phi_3(T_{\max}) = \Delta\phi_1^>$, where we have used the continuity of the applied heat flux at the critical temperature [$\phi_3(T_c^>) = \phi_3(T_{\max})$]. This invariance of the heat-flux jumps during the heating also holds for the cooling ($\Delta\phi_2^< = \Delta\phi_1^<$), regardless of the collector or emitter temperature, and it is shown in Fig. 4.

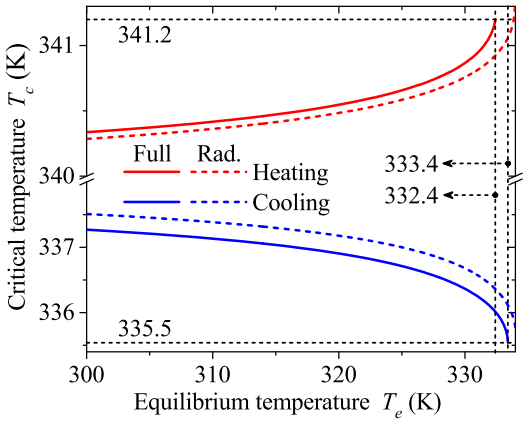

FIG. 5. VO_2 base critical temperature as a function of the equilibrium one T_e. The dashed lines stand for the solution of Eq. (4) for pure radiation ($G = 0$).

According to Fig. 5, as the equilibrium temperature T_e raises, the monotonous increase of the critical temperature $T_c^> \leq 341.2$ K is accompanied by the decrease of $T_c^< \geq 335.5$ K, such that their values fall within the VO_2 transition regions for the heating and cooling regimes (Fig. 2), respectively. For pure heat radiation ($G = 0$), these critical temperatures have similar values to the corresponding ones obtained for $G > 0$, but both of their upper bounds on T_e are shifted to 334 K. The fact that $T_c^> > T_c^<$ indicates that the dielectric-to-metal transition of VO_2 could be more suitable than the metal-to-dielectric one for enhancing the heat fluxes. This is confirmed by Fig. 6, which shows the comparison of the heat fluxes at the critical temperatures. The applied flux ϕ_3 required to reach $T_c^>$ is higher than that for $T_c^<$, and its values reduce as T_e increases. On the other hand, for each T_e, the heat flux $\phi_{2c} > \phi_{1c}$, as established by Eqs. (5b) and (5c), and it remains almost constant. This indicates that ϕ_3 can be

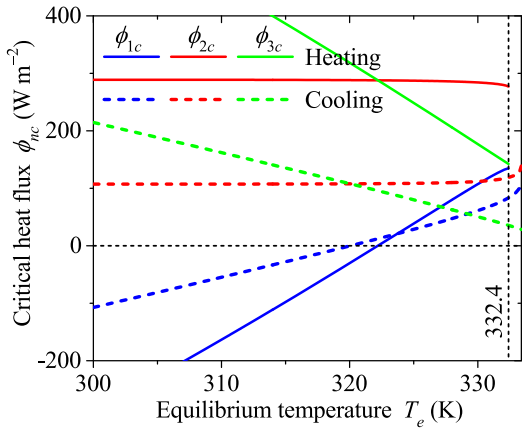

FIG. 6. Dependence of the critical heat fluxes on T_e.

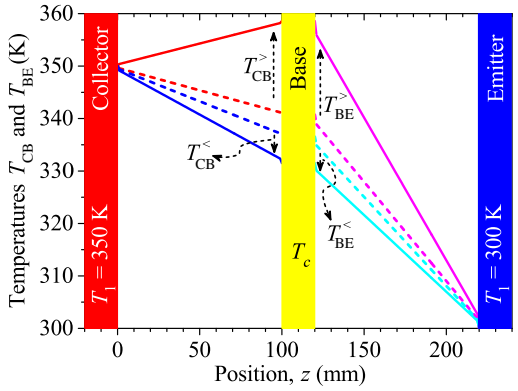

FIG. 7. Spatial distribution of the temperatures T_{CB} and T_{BE} during the heating and cooling of the VO_2 base set at its critical temperature. The vertical arrows stand for the temperature jumps, which are equal on both base surfaces. Calculations are done for an air cavity of thickness $L = 10$ cm and $\delta = 1$ mm.

significantly changed over a wide range of equilibrium temperatures, without modifying the base-to-emitter heat flux. By contrast, the collector-to-base heat flux varies significantly with T_e and its direction can be inverted as T_e reduces. This is caused by the increase of ϕ_3, which can raise the base temperature to values higher than the one ($T_1 = \sqrt[4]{2T_e^4 - T_2^4}$) of the collector. It is therefore clear that to minimize the injected heat flux ϕ_3 and maximize the amplification of ϕ_{1c} and ϕ_{2c} with respect to ϕ_{3c}, T_e has to be set near 332.4 K.

The spatial distributions of the temperatures T_{CB} and T_{BE} are shown in Fig. 7, for both the heating and cooling of the VO_2 base. The temperature changes generated by heat convection near the interfaces are relatively small due to the fact that they occur in very narrow regions ($\delta \ll L$), as described in Eqs. (9) and (10). When heating the transistor base with an applied heat flux $\phi_{3c} = 208$ W m^{-2}, its temperature reaches the critical value $T_c = 340.8$ K and then jumps $+18$ K. During the cooling, on the other hand, as the applied heat flux is reduced to $\phi_{3c} = 63$ W m^{-2}, the base temperature jumps -5 K right after taking its critical value $T_c = 336.6$ K. The temperature jump during the heating is thus larger and requires the application of a higher heat flux than the corresponding one for the cooling. These temperature jumps evidently reduce within the cavities, but they can significantly be enlarged by lowering the equilibrium temperature $T_e = \sqrt[4]{(T_1^4 + T_2^2)/2}$ of the collector and emitter, as shown in Fig. 4.

Control of the transistor base temperature could be applied to heat up or cool down objects placed in the vicinity of the VO_2 base. After setting the temperatures of the collector and emitter with two thermostats, the increase or decrease of the power supplied to the base around its critical values leads to jumps of its temperature up to T_{max} or down to T_{min}, respectively. An object isolated from the environment and in thermal contact with one of the free surfaces of the base, could be kept at a temperature close to T_{max} or T_{min}, if its size is small enough and/or its radiative coupling to the emitter and collector is sufficiently low as to not significantly modify the heat transport within the thermal transistor. The first of these conditions can be fulfilled by samples with sizes much smaller than those of the collector, base, and emitter, while the second one could be satisfied by objects semitransparent to the collector-to-base and base-to-emitter radiative heat fluxes. It is, therefore, clear that the far-field thermal transistor could be used as a device for heating and cooling, as is done with microwave ovens, radiators, and freezers.

IV. CONCLUSIONS

The thermal hysteresis and temperature dependence of the emissivity of a phase-change material have been used to develop a transistorlike device for heating and cooling. Considering the heat currents by radiation, conduction, and convection, an explicit condition for optimizing the transistor amplification factor has been found and used to generate jumps on the base temperature and heat fluxes. For a collector and emitter operating at 350 and 300 K, respectively, a temperature jump of $+18$ K (-5 K) has been obtained during the heating (cooling) of a VO_2 base excited with 208 W m^{-2} (63 W m^{-2}). These sizable jumps show that the proposed transistor could find wide applications in the conception of new thermal devices.

ACKNOWLEDGMENTS

This work was supported by the French Government Program Investissement d'avenir (LABEX INTERACTIFS, ANR-11-LABX-0017-01).

[1] B. Li, L. Wang, and G. Casati, Thermal Diode: Rectification of Heat Flux, Phys. Rev. Lett. **93**, 184301 (2004).
[2] C. R. Otey, W. T. Lau, and S. Fan, Thermal Rectification through Vacuum, Phys. Rev. Lett. **104**, 154301 (2010).
[3] P. Ben-Abdallah and S. A. Biehs, Phase-change radiative thermal diode, Appl. Phys. Lett. **103**, 191907 (2013).
[4] B. Li, L. Wang, and G. Casati, Negative differential thermal resistance and thermal transistor, Appl. Phys. Lett. **88**, 143501 (2006).
[5] P. Ben-Abdallah and S. A. Biehs, Near-Field Thermal Transistor, Phys. Rev. Lett. **112**, 044301 (2014).
[6] P. Ben-Abdallah and S. A. Biehs, Phase-change radiative thermal diode, Appl. Phys. Lett. **103**, 191907 (2013).
[7] K. Joulain, Y. Ezzahri, J. Drevillon, and P. Ben-Abdallah, Modulation and amplification of radiative far field heat transfer: Towards a simple radiative thermal transistor, Appl. Phys. Lett. **106**, 133505 (2015).
[8] N. Li, J. Ren, L. Wang, G. Zhang, P. Hanggi, and B. Li, Phononics, Manipulating heat flow with electronic analogs and beyond, Rev. Mod. Phys. **84**, 1045 (2012).

[9] L. Wang and B. Li, Thermal Logic Gates: Computation with Phonons, Phys. Rev. Lett. **99**, 177208 (2007).

[10] L. Wang and B. Li, Thermal Memory: A Storage of Phononic Information, Phys. Rev. Lett. **101**, 267203 (2008).

[11] V. Kubytskyi, S. A. Biehs, and P. Ben-Abdallah, Radiative Bistability and Thermal Memory, Phys. Rev. Lett. **113**, 074301 (2014).

[12] S. A. Dyakov, J. Dai, M. Yan, and M. Qiu, Near field thermal memory based on radiative phase bistability of VO_2, J. Phys. D **48**, 305104 (2015).

[13] K. Joulain, J. Drevillon, Y. Ezzahri, and J. Ordonez-Miranda, Quantum Thermal Transistor, Phys. Rev. Lett. **116**, 200601 (2016).

[14] M. Terraneo, M. Peyrard, and G. Casati, Controlling the Energy Flow in Nonlinear Lattices: A Model for a Thermal Rectifier, Phys. Rev. Lett. **88**, 094302 (2002).

[15] J. Hu, X. Ruan, and Y. P. Chen, Thermal conductivity and thermal rectification in graphene nanoribbons: A molecular dynamics study, Nano Lett. **9**, 2730 (2009).

[16] E. Pereira, Sufficient conditions for thermal rectification in general graded materials, Phys. Rev. E **83**, 031106 (2011).

[17] G. Zhang and H. Zhang, Thermal conduction and rectification in few-layer graphene *y* junctions, Nanoscale **3**, 4604 (2011).

[18] N. Roberts and D. Walker, A review of thermal rectification observations and models in solid materials, Int. J. Therm. Sci. **50**, 648 (2011).

[19] K. Garcia-Garcia and J. Alvarez-Quintana, Thermal rectification assisted by lattice transitions, Int. J. Therm. Sci. **81**, 76 (2014).

[20] D. Segal, Single Mode Heat Rectifier: Controlling Energy Flow between Electronic Conductors, Phys. Rev. Lett. **100**, 105901 (2008).

[21] H. Iizuka and S. Fan, Rectification of evanescent heat transfer between dielectric-coated and uncoated silicon carbide plates, J. Appl. Phys. **112**, 024304 (2012).

[22] S. Basu and M. Francoeur, Near-field radiative transfer based thermal rectification using doped silicon, Appl. Phys. Lett. **98**, 113106 (2011).

[23] E. Nefzaoui, J. Drevillon, Y. Ezzahri, and K. Joulain, Simple far-field radiative thermal rectifier using Fabry-Perot cavities based infrared selective emitters, Appl. Opt. **53**, 3479 (2014).

[24] K. Joulain, Y. Ezzahri, J. Drevillon, B. Rousseau, and D. De Sousa Menese, Radiative thermal rectification between SiC and SiO_2, Opt. Express **23**, A1388 (2015).

[25] J. Ordonez-Miranda, Y. Ezzahri, J. Drevillon, and K. Joulain, Dynamical heat transport amplification in a far-field thermal transistor of VO_2 excited with a laser of modulated intensity, J. Appl. Phys. **119**, 203105 (2016).

[26] C. W. Chang, D. Okawa, A. Majumdar, and A. Zettl, Solid-state thermal rectifier, Science **314**, 1121 (2006).

[27] R. Scheibner, M. Knig, D. Reuter, A. D. Wieck, C. Gould, H. Buhmann, and L. W. Molenkamp, Quantum dot as thermal rectifier, New J. Phys. **10**, 083016 (2008).

[28] W. Kobayashi, Y. Teraoka, and I. Terasaki, An oxide thermal rectifier, Appl. Phys. Lett. **95**, 171905 (2009).

[29] P. J. van Zwol, L. Ranno, and J. Chevrier, Tuning Near Field Radiative Heat Flux Through Surface Excitations with A Metal Insulator Transition, Phys. Rev. Lett. **108**, 234301 (2012).

[30] P. J. van Zwol, L. Ranno, and J. Chevrier, Emissivity measurements with an atomic force microscope, J. Appl. Phys. **111**, 063110 (2012).

[31] P. J. van Zwol, K. Joulain, P. Ben-Abdallah, and J. Chevrier, Phonon polaritons enhance near-field thermal transfer across the phase transition of VO_2, Phys. Rev. B **84**, 161413(R) (2011).

[32] K. Ito, K. Nishikawa, and H. Lizuka, Thermal conductivity of nano-layered systems due to surface phonon-polaritons, Appl. Phys. Lett. **108**, 053507 (2016).

[33] Y. Yang, S. Basu, and L. Wang, Radiation-based near-field thermal rectification with phase transition materials, Appl. Phys. Lett. **103**, 163101 (2013).

[34] K. Ito, K. Nishikawa, H. Lizuka, and H. Toshiyoshi, Experimental investigation of radiative thermal rectifier using vanadium dioxide, Appl. Phys. Lett. **105**, 253503 (2014).

[35] F. P. Incropera, D. P. Dewitt, T. L. Bergman, and A. S. Lavine, *Fundamentals of Heat and Mass Transfer* (John Wiley & Sons, Hoboken, NJ, 2011).

[36] A. Salazar, R. Fuente, E. Apinaniz, A. Mendioroz, and R. Celorio, Simultaneous measurement of thermal diffusivity and optical absorption coefficient using photothermal radiometry. II Multilayered solids, J. Appl. Phys. **110**, 033516 (2011).

[37] H. Prod'homme, J. Ordonez-Miranda, Y. Ezzahri, J. Drevillon, and K. Joulain, Optimized thermal amplification in a radiative transistor, J. Appl. Phys. **119**, 194502 (2016).

[38] M. M. Qazilbash, M. Brehm, G. O. Andreev, A. Frenzel, P. C. Ho, B. G. Chae, B. J. Kim, S. J. Yun, H. T. Kim, A. V. Balatsky, O. G. Shpyrko, M. B. Maple, F. Keilmann, and D. N. Basov, Infrared spectroscopy and nano-imaging of the insulator-to-metal transition in vanadium dioxide, Phys. Rev. B **79**, 075107 (2009).

[39] M. M. Qazilbash, M. Brehm, B. G. Chae, P. C. Ho, G. O. Andreev, B. J. Kim, S. J. Yun, A. V. Balatsky, M. B. Maple, F. Keilmann, H. T. Kim, and D. N. Basov, Mott transition in VO_2 revealed by infrared spectroscopy and nano-imaging, Science **318**, 1750 (2007).

[40] G. Seo, B. J. Kim, Y. W. Lee, and H. T. Kim, Photo-assisted bistable switching using Mott transition in two-terminal VO_2 device, Appl. Phys. Lett. **100**, 011908 (2012).